

# The miRNA COMPLEXES AGAINST CORONAVIRUSES COVID-19, SARS-CoV, and MERS-CoV

Anatoliy Ivashchenko (✉ [a.iavashchenko@gmail.com](mailto:a.iavashchenko@gmail.com))

al-Farabi Kazakh National University <https://orcid.org/0000-0002-7969-2016>

Aizhan Rakhmetullina

al-Farabi Kazakh National University <https://orcid.org/0000-0002-0117-7110>

Aigul Akimniyazova

al-Farabi Kazakh National University <https://orcid.org/0000-0001-7283-3958>

Dana Aisina

al-Farabi Kazakh National University <https://orcid.org/0000-0002-7137-3408>

Anna Pyrkova

al-Farabi Kazakh National University <https://orcid.org/0000-0001-8483-451X>

---

## Research Article

**Keywords:** miRNA, human, CORONAVIRUSE, COVID-19, SARS-CoV, MERS-CoV

**Posted Date:** March 31st, 2020

**DOI:** <https://doi.org/10.21203/rs.3.rs-19592/v1>

**License:**   This work is licensed under a Creative Commons Attribution 4.0 International License.

[Read Full License](#)

---

# Abstract

The possibility of using miRNA (mRNA-inhibiting RNA) to inhibit infections caused by the coronaviruses COVID-19, SARS-CoV, and MERS-CoV has been shown. Using bioinformatics approaches, completely complementary miRNA (cc-miRNA) complexes were predicted to be able to bind and inhibit the translation of coronavirus proteins and the replication of COVID-19, SARS-CoV, and MERS-CoV genomes. For complexes of seven cc-miRc for COVID-19, seven cc-miRs for SARS-CoV, and eight cc-miRm for MERS-CoV, the interactions with the RNA genomes (gRNAs) of the corresponding coronaviruses was evaluated. The free energy of the interactions of cc-miRNAs with binding sites was significantly higher than the free energy of the interactions with other regions in gRNA, which ensures high selectivity of the binding of cc-miRNAs. Weak binding of cc-miRNAs to the mRNAs of 17508 human genes was shown, which suggests the absence of side effects of the cc-miRNAs in humans. A feature of this method is the simultaneous inhibition of translation and replication by several cc-miRNAs binding from the 5' end to the 3' end of gRNA. The use of several cc-miRNAs to suppress infections allows each of them to be used at a lower concentration to avoid side effects when one cc-miRNA is introduced into humans at a high concentration.

## Introduction

miRNAs (mRNA-inhibiting RNAs) are involved in the regulation of gene expression at the translational level [1]. These nanosized molecules with a length of 6–8 nm can bind to mRNAs with all 19–28 nucleotides, providing high selectivity for interaction with a single gene or several target genes [2,3]. Based on this property of miRNA, attempts have been made to regulate the expression of viral genes using natural miRNAs or by creating synthetic siRNAs [4,5,6]. In some cases, this approach gave a positive result *in vitro* but was not applicable *in vivo* for several reasons, including the lack of evidence that miRNA and siRNA do not have side effects in humans or experimental animals [7,8,9,10]. The basis of our approach to the use of miRNAs in the fight against coronaviruses COVID–19, SARS-CoV, and MERS-CoV is to create completely complementary miRNA (cc-miRNA) that will highly specifically inhibit the translation of viral proteins by strong interactions with the RNA genomes (gRNA) of viruses. Such cc-miRNAs associated with the gRNA of the virus will inhibit genome replication. Thus, two goals are achieved by using cc-miRNA: to stop the synthesis of proteins of the virus that has entered the cell and to inhibit the reproduction of its genome. Such actions of cc-miRNAs on the virus should be highly specific and not have side effects on any human genes.

## Results

The first task of this study was to identify human miRNAs that would have the greatest effect on the expression of the genomes of the coronaviruses COVID-19, SARS-CoV, and MERS-CoV at the translational level. Then, cc-miRNAs were created that could efficiently bind to the gRNA nucleotide sequence at the 5'-end to avoid wasting the resources of the recipient cell on the synthesis of all proteins encoded by the viral genome. Furthermore, cc-miRNAs were also created for other parts of gRNA to enhance translational

inhibition by applying two or more cc- miRs. To inhibit genome replication, we searched for cc-miRNAs with binding sites at the 3' end of gRNA to block replication at the beginning of the process. To assess the side effects of cc- miRNAs in humans, the characteristics of the interactions of cc-miRNAs with the mRNAs of 17508 human genes in our database were determined. In addition, intramolecular interactions of the cc-miRNA binding site with gRNA regions were taken into account.

## Creation of the cc-miRc complex for the gRNA of COVID-19

Despite the large gRNA of COVID-19, in comparison with human protein-coding genes, only a few human miRNAs with a  $\Delta G/\Delta G_m$  of 90% or more could bind to the COVID-19 genome. We chose this  $\Delta G/\Delta G_m$  value as a performance criterion based on the requirement that different miRNAs with a length of 22 nucleotides (nt) are different by two or more nucleotides, which allows them to bind specifically. For example, a decrease in this criterion by 5% leads to an increase in the putative target genes of a particular miRNA by a factor of many, which leads to a large number of false target genes of the miRNA. To create cc-miRc (completely complementary miRNA of COVID-19), we chose ID02510.3p-miR, ID00448.3p-miR, miR-3154, miR-7114-5p, miR-5197-3p, ID02750.3p-miR,

and ID01851.5p-miR, which bind with the gRNA of COVID-19 with  $\Delta G/\Delta G_m$  equal to 89% or more. Furthermore, the length of these miRNAs was increased to 25–27 nt at the 5' and 3' ends of the miRNAs, and noncanonical C-A and G-U pairs were replaced by canonical U-A and G-C pairs to increase the free energy of the interactions of cc-miRc with the gRNA of COVID-19. Table 1 shows the characteristics of the fully complementary interactions of the nucleotides of seven cc-miRc with gRNA. Lengths of 25–28 nt and more have been found among natural miRNAs (miR-1273a, miR-1273d, miR-1272, miR-1292-5p, miR-3143, miR-1226-5p, miR-

7161-3p) and therefore, as part of the RISC (RNA-induced silencing complex), can interact with gRNA. In the gRNA of COVID-19, which has a length of 29903 nt, intramolecular hydrogen bonds are formed that involve cc-miRc binding sites (bs-cc-miRc), which can impede the interaction of cc-miRc with their bs-cc-miRc. The free energy of the intramolecular interactions of bs-cc-miRc is  $-39$  kJ/mole ÷  $-43$  kJ/mole lower than the  $\Delta G$  of their interactions with cc-miRc (Table 1), which indicates their weak influence on the binding of cc-miRc with bs-cc-miRc. The created cc-miRc interacted with the mRNAs of 17508 genes with free energy  $-19$  kJ/mole ÷  $-22$  kJ/mole, that lower than cc-miRc with gRNA (Table 1). This result suggests that each cc-miRc can, when used at adequate concentrations, interact with gRNA without side effects on the human protein-coding genes.

Table 1| Characteristics of the interactions of cc-miRc with gRNA COVID-19 and mRNAs of human genes

RNA	miRNA	Start of site, nt	Region of RNA	$\Delta G$ , kJ/mole	$\Delta G/\Delta G_m$ , %	Length, nt
gRNA	cc-miR1c	193	5'UTR	-149	100	27
gRNA	bs-cc-miR1c	544	CDS	$\leq -106$	$\leq 71$	27
mRNAs	cc-miR1c			$\leq -126$	$\leq 85$	27
gRNA	cc-miR2c	16390	CDS	-144	100	26
gRNA	bsi-cc-miR2c	3157	CDS	$\leq -104$	$\leq 75$	26
mRNAs	cc-miR2c			$\leq -122$	$\leq 85$	26
gRNA	cc-miR3c	17116	CDS	-146	100	27
gRNA	bs-cc-miR3c	253	5'UTR	$\leq -104$	$\leq 71$	27
mRNAs	cc-miR3c			$\leq 125$	$\leq 86$	27
gRNA	cc-miR4c	18101	CDS	-146	100	27
gRNA	bs-cc-miR4c	ND	CDS	$\leq -102$	$\leq 69$	27
mRNAs	cc-miR4c			$\leq 125$	$\leq 86$	27
gRNA	cc-miR5c	21893	CDS	-132	100	25
gRNA	bs-cc-miR5c	20296	CDS	$\leq -93$	$\leq 71$	25
mRNAs	cc-miR5c			$\leq -112$	$\leq 85$	25
gRNA	cc-miR6c	28359	CDS	-140	100	25
gRNA	bs-cc-miR6c	15100	CDS	$\leq -100$	$\leq 71$	25
mRNAs	cc-miR6c			$\leq -119$	$\leq 85$	25
gRNA	cc-miR7c	28883	CDS	-146	100	27
gRNA	bs-cc-miR7c	23076	CDS	$\leq -104$	$\leq 71$	27
mRNAs	cc-miR7c			$\leq -124$	$\leq 85$	27

Note. cc-miR1c - cc-miR7c are cc-miRc created on the basis of ID02510,3p-miR (1), ID00448,3p-miR (2), miR-3154 (3), miR-7114-5p (4), miR-5197-3p (5), ID02750,3p-miR (6), ID01851,5p-miR (7), respectively.

The interaction schemes of the seven cc-miRc complexes with the corresponding bs-cc-miRc on the gRNA of COVID-19 are shown in Fig. 1. These interaction schemes of cc-miRc with binding sites in gRNA were predicted by the MirTarget program, and quantitative characteristics of interactions are shown in Table 1. In the interaction schemes of bs-cc-miRc with gRNA, there were only completely complementary bindings of all nucleotides, and there were no non-canonical A-C and G-U pairs, which was confirmed by a  $\Delta G/\Delta G_m$  value of 100%.

## Creation of the cc-miRm complex for the gRNA of MERS-CoV

The size of the gRNA of MERS-CoV is 30119 nt, which is several times larger than the average size of the mRNA of human genes. Only a few human miRNAs with a  $\Delta G/\Delta G_m$  value of 89% or more could bind with the MERS-CoV genome. To create cc-miRm (completely complementary miRNA of MERS-CoV) for MERS-CoV, we chose miR-3976, ID02684,5p-miR, miR-3591-3p, ID02892,3p-miR, ID02389,3p-miR, miR-1271-3p, and ID00939,5p-miR, which bind with gRNA of MERS-CoV with a  $\Delta G/\Delta G_m$  value of 89% or less.

Furthermore, the length of these miRNAs was increased to 25–27 nt at the 5' and 3' ends of the miRNAs, and non-canonical A-C and G-U pairs were replaced by canonical U-A and G-C pairs to increase the free energy of the interaction of cc-miRm with the gRNA of MERS-CoV. Table 2 shows the characteristics of the fully complementary interactions of the nucleotides of seven cc-miRm with gRNA. Lengths of 25–27 nt, as mentioned above, are found among natural miRNAs and therefore, as part of the RISC, these miRNAs can interact with gRNA. Intramolecular hydrogen bonds are formed in the gRNA of MERS-CoV with the participation of bs-cc-miRm binding sites, which can impede the interaction of cc-miRm with their bs-cc-miRm. The free energy of the intramolecular interactions of bs-cc-miRm is -30 kJ/mole ÷ -46 kJ/mole, that lower than the  $\Delta G$  of their interaction with cc-miRm (Table 2), which indicates the weak influence of their intramolecular interactions on the binding of cc-miRm with bs-cc-miRm. The created cc-miRm interacted with mRNA of 17508 genes with free energy -20 kJ/mole ÷ -22 kJ/mole lower than cc-miRm with gRNA (Table 2). This result indicates that each cc-miRm, used at adequate concentrations, can interact with gRNA without side effects on the human protein-coding genes.

Table 2| Characteristics of the interactions of cc-miRm with the gRNA of MERS-CoV and mRNAs of human genes

RNA	miRNA	Start of site, nt	Region of RNA	$\Delta G$ , kJ/mole	$\Delta G/\Delta G_m$ , %	Length, nt
gRNA	cc-miR1m	123	CDS	-142	100	27
gRNA	bs-cc-miR1m	24648	CDS	$\leq -112$	$\leq 79$	27
mRNAs	cc-miR1m		CDS	$\leq -120$	$\leq 85$	27
gRNA	cc-miR2m	515	CDS	-144	100	26
gRNA	bs-cc-miR2m	8742	CDS	$\leq -102$	$\leq 71$	26
mRNAs	cc-miR2m			$\leq -122$	$\leq 85$	26
gRNA	cc-miR3m	3164	CDS	-151	100	27
gRNA	bs-cc-miR3m	12492	CDS	$\leq -105$	$\leq 70$	27
mRNAs	cc-miR3m			$\leq -129$	$\leq 86$	27
gRNA	cc-miR4m	10236	CDS	-138	100	25
gRNA	bs-cc-miR4m	236	CDS	$\leq -99$	$\leq 72$	25
mRNAs	cc-miR4m			$\leq -117$	$\leq 85$	25
gRNA	cc-miR5m	13796	CDS	-136	100	26
gRNA	bs-cc-miR5m	12614	CDS	$\leq -102$	$\leq 75$	26
mRNAs	cc-miR5m			$\leq -116$	$\leq 85$	26
gRNA	cc-miR6m	24307	CDS	-142	100	26
gRNA	bs-cc-miR6m	9997	CDS	$\leq -103$	$\leq 73$	26
mRNAs	cc-miR6m			$\leq -120$	$\leq 85$	26
gRNA	cc-miR7m	28342	CDS	-146	100	27
mgRNA	bs-cc-miR7m	13480	CDS	$\leq -111$	$\leq 79$	27
mRNAs	cc-miR7m			$\leq -126$	$\leq 86$	27

Note. cc-miR1m - cc-miR7m are cc-miRm created on the basis of miR-3976 (1), ID02684.5p-miR (2), miR-3591-3p (3), ID02892.3p-miR (4), ID02389.3p-miR (5), miR-1271-3p (6), ID00939.5p-miR (7), respectively.

The interaction schemes of the complex of seven cc-miRm with the corresponding bs-cc-miRm on the gRNA of MERS-CoV are shown in Fig. 2. These interaction schemes of cc-miRm with binding sites in

gRNA were predicted by the MirTarget program, and quantitative characteristics of interactions are shown in Table. 2.

## Creation of the cc-miRs complex for the gRNA of SARS-CoV

Despite the large gRNA of SARS-CoV, which is 29751 nt long, compared with that of human protein-coding genes, only a few human miRNAs with  $\Delta G/\Delta G_m$  of 89% or more could bind to the SARS-CoV genome. To create cc-miRs, we chose ID00322.5p-miR, miR-20b-3p, miR-497-3p, ID01820.3p-miR, miR-505-3p, ID00749.3p-miR, ID03254.5p-miR, and ID00271.5p-miR, which bound with the gRNA of SARS-CoV with a  $\Delta G/\Delta G_m$  value equal to 89% or less. The length of these miRNAs was increased to 25–28 nt at the 5' and 3' ends of the miRNAs, and non-canonical C-A and G-U pairs were replaced by canonical U-A and G-C pairs to increase the free energy of the interaction of cc-miRs with the gRNA of SARS-CoV. Table 3 shows the characteristics of the fully complementary interactions of the nucleotides of eight cc-miRs with gRNA. Intramolecular hydrogen bonds involving bs-cc-miRs are formed in the gRNA of SARS-CoV, which can impede the interaction of cc-miRs with their bs-cc-miRs. The free energy of the intramolecular interactions of bs-cc-miRs is  $-34$  kJ/mole  $\div$   $-44$  kJ/mole lower than the  $\Delta G$  of their interaction with cc-miRs (Table 3), which indicates a weak effect of the intramolecular interactions on the binding of cc-miRs to bs-cc-miRs. The created cc-miRs interacted with the mRNAs of 17508 genes with free energy  $-19$  kJ/mole  $\div$   $-24$  kJ/mole lower than cc-miRs with gRNA (Table 3). This result suggests that each cc-miRs at concentrations comparable with the concentrations of endogenous miRNA can interact with gRNA without side effects on the human protein-coding genes.

Table 3| Characteristics of the interactions of cc-miRs with the gRNA SARS-CoV and mRNAs of human genes

RNA	miRNA	Start of site, nt	Region of RNA	$\Delta G$ , kJ/mole	$\Delta G/\Delta G_m$ , %	Length, nt
gRNA	cc-miR1s	91	5'UTR	-153	100	27
gRNA	bs-cc-miR1s	746	CDS	$\leq -113$	$\leq 74$	27
mRNAs	cc-miR1s			$\leq -133$	$\leq 87$	27
gRNA	cc-miR2s	574	CDS	-157	100	28
gRNA	bs-cc-miR2s	16058	CDS	$\leq -113$	$\leq 72$	28
mRNAs	cc-miR2s			$\leq -133$	$\leq 85$	28
gRNA	cc-miR3s	1849	CDS	-140	100	27
gRNA	bs-cc-miR3s	15403	CDS	$\leq -106$	$\leq 76$	27
mRNAs	cc-miR3s			$\leq -120$	$\leq 86$	27
gRNA	cc-miR4s	2058	CDS	-136	100	26
gRNA	bsi-cc-miR4s	11658	CDS	$\leq -99$	$\leq 73$	26
mRNAs	cc-miR4s			$\leq -117$	$\leq 86$	26
gRNA	cc-miR5s	12482	CDS	-144	100	27
gRNA	bs-cc-miR5s	20270	CDS	$\leq -103$	$\leq 72$	27
mRNAs	cc-miR5s			$\leq -123$	$\leq 86$	27
gRNA	cc-miR6s	19145	CDS	-142	100	27
gRNA	bs-cc-miR6s	18037	CDS	$\leq -99$	$\leq 70$	27
mRNAs	cc-miR6s			$\leq -121$	$\leq 85$	27
gRNA	cc-miR7s	21142	CDS	-142	100	27
gRNA	bs-cc-miR7s	17101	CDS	$\leq -104$	$\leq 73$	27
mRNAs	cc-miR7s			$\leq -121$	$\leq 85$	27
gRNA	cc-miR8s	27316	CDS	-142	100	27
gRNA	bs-cc-miR8s	21548	CDS	$\leq -104$	$\leq 73$	27
mRNAs	cc-miR8s			$\leq -121$	$\leq 85$	27

Note. cc-miR1s - cc-miR7s are cc-miRs created on the basis of ID00322.5p-miR (1), miR-20b-3p (2), miR-497-3p (3), ID01820.3p-miR (4), miR-505-3p (5), ID00749.3p-miR (6), ID03254.5p-miR (7), ID00271.5p-miR (8), respectively.

The interaction schemes of the complex of eight cc-miRm with the corresponding bs-cc-miRm on the gRNA of SARS-CoV are shown in Fig. 3. These interaction schemes of cc-miRm with binding sites in gRNA were predicted by the MirTarget program, and quantitative characteristics of interactions are shown in Table. 3.

## Synthesis and delivery of cc-miRNAs into humans

The synthesis of cc-miRNAs is an inexpensive procedure - in terms of cost, it corresponds to the synthesis of primers. Our hypothesis can be tested in laboratories with the right and ability to conduct inexpensive and short-term tests proposed by cc-miRNAs as a means of combating COVID-19, SARS-CoV, and MERS-CoV coronaviruses. Since the size of cc-miRNAs is approximately 9 nm, they can be delivered via circulation to many organs as part of ordinary exosomes in human blood measuring 30–150 nm

[11,12,13]. As part of exosomes, cc-miRNAs can be introduced into the lung by inhalation. The proposed method of combating coronavirus does not have toxicity or side effects. cc-miRNAs are susceptible to degradation by nucleases, similar to all human miRNAs, and the removal of cc-miRNAs from the body is not difficult. In the absence of side effects, cc-miRNAs can be used as a therapeutic agent.

## Conclusion

The nucleotide sequences of the cc-miRNAs were created based on known miRNAs and on their binding sites in the gRNA of COVID-19, SARS-CoV, and MERS-CoV. The binding characteristics of cc-miRNAs and their complementary nucleotide sequence (as a pre-miRNA) on mRNAs of human genes were determined to identify side effects of cc-miRNAs on human gene expression. The use of a complex of several miRNAs to suppress coronavirus infection allows the inhibition of viral protein synthesis and gRNA replication; reduces the toxicity of each cc-miRNA by allowing the use of concentrations equal to those of endogenous miRNA; quickly spreads via circulations to many organs; and is excreted from organisms as are all endogenous miRNAs. The proposed method does not require a large number of reagents and is not time consuming. The cc-miRNAs can be used as a therapeutic agents for coronavirus infections with COVID-19, SARS-CoV, and MERS-CoV.

## Methods

The nucleotide sequences of 2565 miRNAs were downloaded from miRBase (<http://mirbase.org>, Release 22.1). Another 3307 miRNAs were obtained from the article by Londin et al. [14]. The nucleotide sequences of human genes and coronavirus COVID-19, SARS-CoV, and MERS-CoV genomes were obtained from GenBank (<http://www.ncbi.nlm.nih.gov>). A search for the target genes of miRNAs was performed using the MirTarget program [15,16,17]. This program determines the following binding characteristics: the start of the miRNA binding site on the mRNA; the locations of the miRNA binding sites in the 3'UTR, 5'UTR, or CDS; the interaction free energy ( $\Delta G$ , kJ/mole); and nucleotide interaction schemes between miRNAs and mRNAs. The ratio of  $\Delta G/\Delta G_m$  (%) was determined for each binding site, where  $\Delta G_m$  is equal to the free energy of the binding of miRNA with its fully complementary nucleotide sequence. The MirTarget program looks for hydrogen bonds between adenine (A) and uracil (U), guanine (G) and cytosine (C), G and U, and A and C [18]. The distances between A and C are equal to 1.04 nanometers, between G and C, and A and U are equal to 1.03 nanometers, between G and U are equal to 1.02 nanometers [17]. The numbers of hydrogen bonds in the G-C, A-U, G-U and A-C interactions were 3, 2, 1 and 1, respectively [16,17].

## Declarations

### Acknowledgments

All authors designed the research and wrote the paper.

## Funding

This study was supported by a grant (AP05132460) from the Ministry of Education and Science, Kazakhstan Republic, SRI of Biology and Biotechnology Problems, al-Farabi Kazakh National University.

## References

1. Bartel, D. P. Metazoan MicroRNAs. *Cell* **173**, 20-51 (2018).
2. Atambayeva, S. *et al.* The Binding Sites of miR-619-5p in the mRNAs of Human and Orthologous Genes. *BMC Genomics* **18**, 428 (2017).
3. Kondybayeva, A. M., Akimniyazova, A. N., Kamenova, S. U., Ivashchenko, A. T. The characteristics of miRNA binding sites in mRNA of ZFH3 gene and its orthologs. *Vavilov journal of Genetics and Breeding* **22**, 438-444 (2018).
4. Ma, Y. *et al.* The Coronavirus Transmissible Gastroenteritis Virus Evades the Type I Interferon Response through IRE1 $\alpha$ -Mediated Manipulation of the MicroRNA miR-30a- 5p/SOCS1/3 Axis. *J Virol.* **92**, e00728-18 (2018).
5. Nur, S. M., Hasan, M. A., Amin, M. A., Hossain, M., Sharmin, T. Design of Potential RNAi (miRNA and siRNA) Molecules for Middle East Respiratory Syndrome Coronavirus (MERS- CoV) Gene Silencing by Computational Method. *Interdiscip Sci.* **7**, 257-65 (2015).
6. Mallick, B., Ghosh, Z., Chakrabarti, J. MicroRNome analysis unravels the molecular basis of SARS infection in bronchoalveolar stem cells. *PLoS One* **4**, e7837 (2009)
7. Dickey, L. L., Worne, C. L., Glover, J. L., Lane, T. E., O'Connell, R.M. MicroRNA-155 enhances T cell trafficking and antiviral effector function in a model of coronavirus-induced neurologic disease. *J Neuroinflammation* **13**, 240 (2016).
8. Hasan, M. M., Akter, R., Ullah, M. S., Abedin, M. J., Ullah, G. M., Hossain, M. Z. A Computational Approach for Predicting Role of Human MicroRNAs in MERS-CoV Genome. *Adv Bioinformatics* **2014** (2014).
9. Zhang, Y. *et al.* Silencing SARS-CoV Spike protein expression in cultured cells by RNA interference. *FEBS Lett.* **560**, 141-6 (2004).
10. Lai, F. W., Stephenson, K. B., Mahony, J., Lichty, B.D. Human coronavirus OC43 nucleocapsid protein binds microRNA 9 and potentiates NF- $\kappa$ B activation. *J Virol.* **88**, 54-65 (2014).
11. Zhang, Zh., Dombroski, J. A., King, M. R. Engineering of Exosomes to Target Cancer Metastasis. *Cellular and Molecular Bioengineering* **13**, 1-16 (2020).
12. Herrera-Carrillo, E., Liu, Y. P. Berkhout B. Improving miRNA delivery by optimizing mirna expression cassettes in diverse virus vectors. *Human Gene Therapy Methods* **28**, 177-190 (2017).
13. Song, X. *et al.* Transmissible gastroenteritis virus (TGEV) infection alters the expression of cellular microRNA species that affect transcription of TGEV gene 7. *Int J Biol Sci.* **11**, 913-22 (2015).

14. Londin, E. *et al.* Analysis of 13 cell types reveals evidence for the expression of numerous novel primate- and tissue-specific microRNAs. *PNAS USA* **112**, 1106-1115 (2015).
15. Ivashchenko, A., Pyrkova, A., Niyazova, R. A method for clustering of miRNA sequences using fragmented programming. *Bioinformatics* **1**, 15-18 (2016).
16. Kool, E. T. Hydrogen bonding, base stacking, and steric effects in DNA replication. *Annual Review of Biophysics and Biomolecular Structure* **30**, 1-22 (2001).
17. Leontis, N. B., Stombaugh, J., Westhof, E. The non-Watson-Crick base pairs and their associated isostericity matrices. *Nucleic Acids Research* **30**, 3497-3531 (2002).
18. Garg, A., Heinemann, U. A novel form of RNA double helix based on G·U and C·A+ wobble base pairing. *RNA* **24**, 209-218 (2018).

## Figures

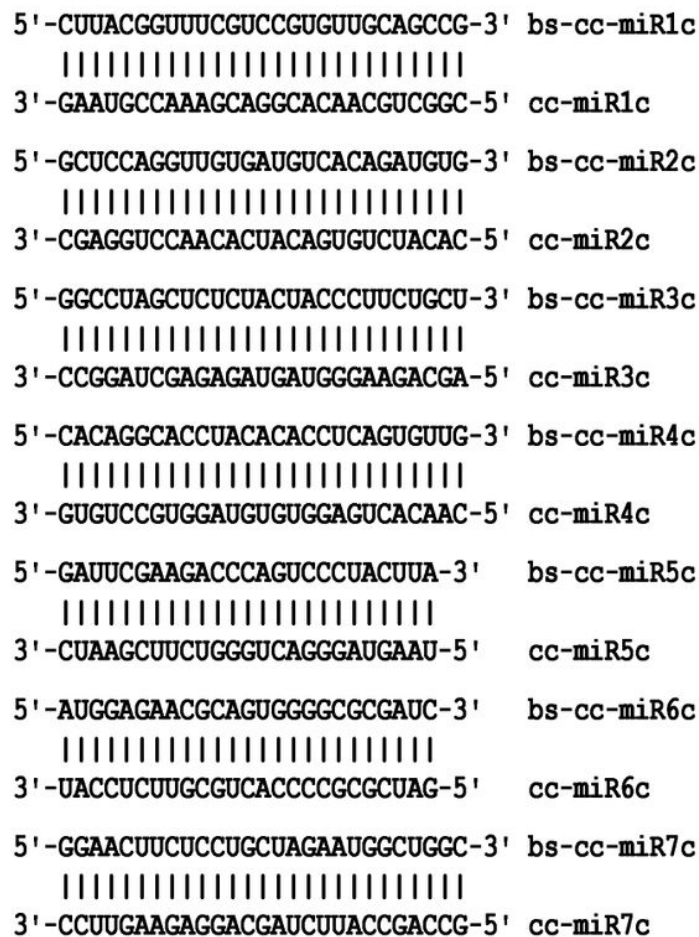


Figure 1

Schemes of the interaction of the cc-miRc complex with the corresponding bs-cc-miRc on the gRNA of COVID-19.

```

5'-GGCAUUAUUUGCCUGCUCAUCUAGGC-3' bs-cc-miR1m
|||||
3'-CCGUAAUUAACGGACGAGUAGAUCCG-5' cc-miR1m

5'-CACUAGACACCUCCAGGUCCUCGUG-3' bs-cc-miR2m
|||||
3'-GUGAUCUGUGGAGGGUCCAGGAGCAC-5' cc-miR2m

5'-CCCCGUCGAGUGUGACGAGGAGUGUUC-3' bs-cc-miR3m
|||||
3'-GGGGCAGCUCACACUGCUCCUCAAG-5' cc-miR3m

5'-GGCGCUCCAGCAAACUUGCGUGUUG-3' bs-cc-miR4m
|||||
3'-CCGCGAGGUCGUUUGAACGCACAAC-5' cc-miR4m

5'-GUUAUAGCCUGAGGCACUUUGAUCA-3' bs-cc-miR5m
|||||
3'-CAUAUACGGGACUCCGUGAAACUAGU-5' cc-miR5m

5'-UGCUUGGCAGCAUAGCAGGUGUUGGC-3' bs-cc-miR6m
|||||
3'-ACGAACCGUCGUAUCGUCCACAACCG-5' cc-miR6m

5'-CCUAUGAAGUCACCGUGGCCAAACCC-3' bs-cc-miR7m
|||||
3'-GGAUUACUUCAGUGGCACCGGUUUGG-5' cc-miR7m

```

**Figure 2**

Schemes of the interaction of the cc-miRm complex with the corresponding bs-cc-miRm on the gRNA of MERS-CoV.

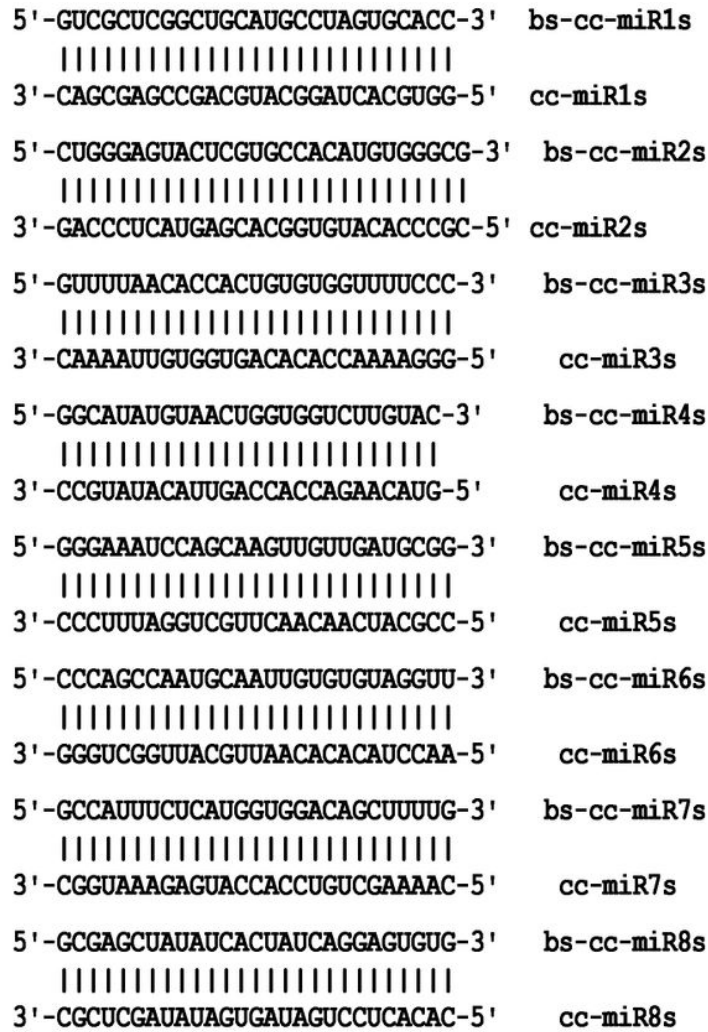


**Figure 3**

Schemes of the interaction of the cc-miRs complex with the corresponding bs-cc-miRs on the gRNA of SARS-CoV.

## Supplementary Files

This is a list of supplementary files associated with this preprint. Click to download.

- [ThemIRNACOMPLEXESAGAINSTCORONAVIRUSESCOVID19SARSCoVandMERSCoV.pdf](#)